

# Development of Biocompatible Coatings with PVA/Gelatin Hydrogel Films on Vancomycin-Loaded Titania Nanotubes for Controllable Drug Release

Thitima Wattanavijitkul, Jirapon Khamwannah, Boonrat Lohwongwatana, Chedtha Puncreobutr, Narendra Reddy, Rungnapha Yamdech, Sarocha Cherdchom, and Pornanong Aramwit\*



Cite This: *ACS Omega* 2024, 9, 37052–37062



Read Online

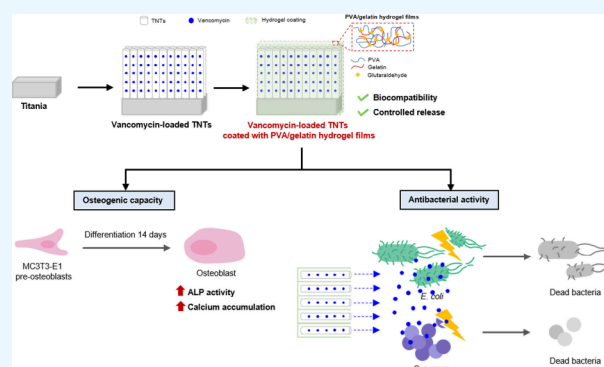
ACCESS |

Metrics & More

Article Recommendations

Supporting Information

**ABSTRACT:** This study investigates the utilization of poly(vinyl alcohol) (PVA)/gelatin hydrogel films cross-linked with glutaraldehyde as a novel material to coat the surface of vancomycin-loaded titania nanotubes (TNTs), with a focus on enhancing biocompatibility and achieving controlled vancomycin release. Hydrogel films have emerged as promising candidates in tissue engineering and drug-delivery systems due to their versatile properties. The development of these hydrogel films involved varying the proportions of PVA, gelatin, and glutaraldehyde to achieve the desired properties, including the gel fraction, swelling behavior, biocompatibility, and biodegradation. Among the formulations tested, the hydrogel with a PVA-to-gelatin ratio of 25:75 and 0.2% glutaraldehyde was selected to coat vancomycin-loaded TNTs. The coated TNTs demonstrated slower release of vancomycin compared with the uncoated TNTs. In addition, the coated TNTs demonstrated the ability to promote osteogenesis, as evidenced by increased alkaline phosphatase activity and calcium accumulation. The vancomycin-loaded TNTs coated with hydrogel film demonstrated effectiveness against both *E. coli* and *S. aureus*. These findings highlight the potential benefits and therapeutic applications of using hydrogel films to coat implant materials, offering efficient drug delivery and controlled release. This study contributes valuable insights into the development of alternative materials for medical applications, thereby advancing the field of biomaterials and drug delivery systems.



## 1. INTRODUCTION

Bone implants are indispensable tools in the rehabilitation process for individuals who have lost body structures due to injury, disease, or congenital abnormalities. These implants serve as substitutes for damaged or missing bones, offering both structural support and functional restoration. The restoration of skeletal integrity is crucial to improve mobility, function, and quality of life.<sup>1</sup> Among the materials explored for medical implant applications, metallic materials such as titanium have emerged as effective biomaterials for bone regeneration and repair.<sup>2–4</sup>

Titanium has emerged as a medical implant material due to its exceptional properties.<sup>5</sup> Its unique combination of strength, lightness, and biocompatibility allow it to be utilized in a wide range of medical implants, ranging from orthopedic surgery to dental prosthetics and cardiovascular devices.<sup>6</sup> Titanium integrates seamlessly with the human body's tissues, promoting osseointegration and ensuring long-term stability and functionality. Moreover, the adaptability of titanium allows for the fabrication of customized implants tailored to each patient's needs, further enhancing their efficacy and precision.<sup>7</sup> As a result, titanium-based materials have become integral compo-

nents in the development of implants aimed at restoring lost or damaged body structures. Despite these advantages, titanium implants are not without limitations, with the risk of infection being a significant concern due to titanium's lack of inherent antibacterial properties.<sup>8</sup> Bacteria can adhere to the surface of titanium implants and form biofilms, resulting in infectious issues.<sup>5</sup> Therefore, researchers are actively exploring strategies such as surface modifications and coatings to enhance the antibacterial properties of titanium implants and to alleviate the risk of infection.

One innovative approach involves the use of vancomycin-loaded titania nanotubes (TNTs) coated with hydrogel films. Hydrogels, which can be derived from natural, synthetic, or hybrid polymers, offer a versatile platform for biomedical

**Received:** April 24, 2024

**Revised:** June 27, 2024

**Accepted:** August 15, 2024

**Published:** August 22, 2024



applications.<sup>9</sup> Among these, poly(vinyl alcohol) (PVA)/gelatin hydrogel films represent a promising biomaterial that combine the beneficial properties of both synthetic and natural polymers.<sup>10,11</sup> PVA/gelatin hydrogels have shown great potential in tissue engineering applications, enhancing cell proliferation and differentiation while exhibiting excellent biocompatibility, high water content, and swellability, and the ability to mimic the natural extracellular matrix and to provide a conducive environment for cellular activities and tissue regeneration.<sup>12–14</sup> Vancomycin can potently reduce the risk of biofilm formation and implant-associated infections.<sup>15,16</sup> The incorporation of vancomycin in bone implant materials represents a promising advancement in the field of orthopedic implantology, offering a potential solution to the persistent challenge of implant-related infections.

In this study, PVA/gelatin hydrogel films were developed to achieve an optimum formulation to coat the surface of TNTs. This study is pioneering in utilizing a PVA/gelatin hydrogel to coat vancomycin-loaded TNTs. The fabrication process involved the synthesis and characterization of hydrogel films, including assessments of the gel fraction, swelling behavior, chemical composition, and biological properties. Subsequently, the hydrogel films were applied to the surface of TNTs via a simple coating process. Extensive investigations were conducted to comprehensively evaluate vancomycin release and their potential utility in treating TNTs. The application of these hydrogel films as coatings on vancomycin-loaded TNTs presents a versatile and effective solution for enhancing the biocompatibility, antibacterial properties, and clinical performance of titanium implants in orthopedic surgery and various other biomedical applications.

## 2. MATERIALS AND METHODS

**2.1. Preparation of Hydrogel Films.** The films were produced by dissolving gelatin (G) (gelatin type A, molecular weight [MW] 15,000–400,000, gel strength [Bloom] 300) in deionized (DI) water (10 wt % gelatin) at 40 °C for 1 h. At the same time, PVA low viscosity (PL) (Merck, Germany, MW 31,000) and PVA high viscosity (PH) (Merck, Germany, MW 205,000) solutions were prepared in DI water (10 wt % PVA) with various ratios at 80 °C and with constant stirring. Then, the PVA and gelatin solutions were mixed at 40 °C for 5 min. After that, glutaraldehyde (GTA) (Ajax Finechem, Australia) was added, and the solution was incubated at 40 °C for 5 min under constant stirring to obtain the PVA/gelatin cross-linked with glutaraldehyde. The solution was poured into a polystyrene plate and incubated at 4 °C for 20 h. The PVA-gelatin films were washed to remove excess glutaraldehyde by soaking in 0.1 mol/L glycine solution for 15 min and then rinsed four times with DI water. Finally, the resulting film-forming solutions were dried at 30 °C for 24–28 h in an air circulatory oven to obtain transparent and flexible films. Table S summarizes the combinations and concentrations of the chemicals used to produce gelatin/PVA hydrogel films.

**2.2. Gel Fraction.** The gel fraction was evaluated on hydrogel film samples with a diameter of 1 cm. The samples were dried for 24 h at 50 °C in an oven (BE 400, Memmert, Germany) and then soaked in DI water at 37 °C for 72 h. The samples were removed from the water and dried again for 24 h at 50 °C in an oven. The gel fraction percentage was calculated as follows:

$$\% \text{ Gel fraction} = \frac{w_e}{W_0} \times 100$$

where  $W_e$  is the weight of the hydrogel film sample dried at 50 °C after soaking in DI water, and  $W_0$  is the initial weight of the hydrogel film sample dried for 24 h at 50 °C.

**2.3. Swelling Behavior.** The films were weighed and immersed in phosphate-buffered saline (PBS, pH 7.4) at 37 °C for 24 h. Subsequently, the swollen product was carefully removed with the aid of a piece of tissue paper, and the mass was measured again. The equilibrium percentage of swelling of the product was calculated as follows:

$$\% \text{ Swelling} = \frac{w_e - w_d}{W_d} \times 100$$

where  $W_e$  is the weight of the product after hydration for 24 h, and  $W_d$  is the mass of the hydrogel film at the beginning of the experiment.

**2.4. Fourier-Transform Infrared (FTIR) Spectroscopy.** FTIR spectra were recorded by using a Spectrum One spectrometer (PerkinElmer, USA). The spectra were recorded between 4000 and 400  $\text{cm}^{-1}$  with a spectral resolution of 4  $\text{cm}^{-1}$ . The data were analyzed with the FTIR Spectrum Software (PerkinElmer). Measurements were performed at room temperature.

**2.5. Scanning Electron Microscopy (SEM).** The surface morphology and thickness of the hydrogel films were evaluated by using SEM (SEM-JSM-IT500HR, JEOL, Japan). The thickness measurements were analyzed by using the ImageJ software (National Institutes of Health, USA).

**2.6. In Vitro Degradation.** The degradation behavior of the hydrogel films was investigated by immersing the hydrogel film samples (1 × 1  $\text{cm}^2$ ) into PBS (pH 7.4, 37 °C) with lysozyme (1.6  $\mu\text{g}/\text{mL}$ ) for 2 weeks. The medium was replaced at 1, 3, 7, 10, and 14 days after sampling with fresh medium. The samples were removed from the degradation medium, washed with distilled water, and excess water on the surface was removed with a piece of filter paper. The samples were transferred to an oven and dried at 60 °C for 24 h to determine the weight loss. The percentage of weight remaining was calculated as follows:

$$\% \text{ Weight remaining} = \frac{w_t}{W_0} \times 100$$

where  $W_t$  is the weight of the hydrogel film sample dried at 60 °C after soaking in degradation medium at different time intervals and  $W_0$  is the initial weight of the hydrogel film sample.

**2.7. Drug Release Study.** To assess the *in vitro* release of vancomycin, uncoated TNTs and TNTs coated with hydrogel films incorporating vancomycin (5 × 5 mm) were suspended in 1 mL of PBS (pH 7.4) and maintained at 37 °C. At predetermined time intervals, 500- $\mu\text{L}$  aliquots were withdrawn and immediately replaced with an equal volume of fresh PBS to ensure a constant volume throughout the experiment. The vancomycin concentration in the collected fractions (taken at different time points) was determined by using a spectrometric microplate reader. The amount of vancomycin released was determined by comparison with a vancomycin standard curve.

**2.8. Determination of Glutaraldehyde Release.** The release of free glutaraldehyde from the hydrogel films into solution was determined by using the MBTH method,<sup>17</sup> with modifications. Briefly, 10 mg of hydrogel film was added to 1

mL of PBS containing the enzyme elastase (1  $\mu\text{g}/\text{mL}$ ) (Wako, Japan) for 24 h until the film was completely dissolved to measure the amount of glutaraldehyde. The extracted solution was mixed with MBTH and  $\text{FeCl}_3$  solutions. The mixed solution was incubated at 25  $^\circ\text{C}$  for 15 min, and then the absorbance at 610 nm was measured by using a spectrometric microplate reader. The amount of glutaraldehyde was determined from a standard curve.

**2.9. Cell Culture.** L929 mouse fibroblasts were grown in Dulbecco's Modified Eagle's Medium (DMEM) supplemented with 10% (v/v) fetal bovine serum and 1% gentamycin (Gibco, USA). The cells were maintained in an atmosphere of 5%  $\text{CO}_2$  at 37  $^\circ\text{C}$ .

**2.10. Cytotoxicity Evaluation.** Each hydrogel film sample (10 mg/mL) was incubated in serum-free medium for 24 h. The extract, containing the products that leached out of the film, was filtered through a 0.22- $\mu\text{m}$  filter and used to assess cell viability with the MTT assay. Briefly,  $1 \times 10^4$  L929 cells were seeded in a 96-well plate at 37  $^\circ\text{C}$  in a humidified atmosphere containing 5%  $\text{CO}_2$  for 24 h. These cells were exposed to varying concentrations of hydrogel extracts for 24 h. The MTT assay was performed as per the standard protocol. The absorbance was measured by using a spectrometric microplate reader. Morphological images were examined with an inverted microscope (Nikon TS2, Japan).

**2.11. Osteoblast Assays.** **2.11.1. Osteoblast Viability.** The viability and growth of osteoblasts were assessed by using the Cell Counting Kit 8 (WST-8/CCK8) (ab228554, Abcam). MC3T3-E1 cells were seeded at a density of  $8 \times 10^4$  cells/well in 6-well plates. The cells were exposed to TNTs, uncoated or coated with hydrogel film, for 24 and 48 h to evaluate toxicity. To observe cell growth on TNTs, MC3T3-E1 cells were seeded on the TNT surface. Subsequently, MC3T3-E1 cells on TNTs, uncoated or coated with hydrogel film, were cultured for 1, 3, and/or 7 days. Afterward, a mixture of 3% CCK8 solution and culture medium was added to each well, followed by incubation for 3 h. Then, the absorbance at 460 nm was measured with a spectrophotometric microplate reader.

**2.11.2. Alkaline Phosphatase (ALP) Activity.** MC3T3-E1 cells were cultured on TNTs, uncoated or coated with hydrogel film, for 14 days in osteogenic differentiation medium ( $\alpha$ -MEM supplemented with 10 mM  $\beta$ -glycerophosphate sodium, 0.05 mM L-ascorbic acid, and 100 mM dexamethasone). Subsequently, the cells were lysed using sodium dodecyl sulfate (SDS) lysis buffer. The ALP activity in the lysate was measured by using *p*-nitrophenyl phosphate at 405 nm with a spectrophotometric microplate reader.

**2.11.3. Intracellular Calcium Content Assay.** After culturing for 3, 7, and 14 days with osteogenic differentiation medium, the calcium content (a late osteogenic marker) was measured in the cell lysate. The 100  $\mu\text{L}$  of cell lysates were mixed with an equal volume of 1 M hydrochloric acid (HCl) and incubated at 37  $^\circ\text{C}$  for 4 h. Subsequently, 10  $\mu\text{L}$  of sample was mixed with 1 mL of 0.88 M ethanolamine buffer (pH 11) and 100  $\mu\text{L}$  of *O*-cresolphthalein complex substrate (OCPC). The absorbance at 570 nm was measured with a spectrometric microplate reader.

**2.12. Antibacterial Assay.** The assay was modified from a previous study.<sup>18</sup> Briefly, the antibacterial ability was evaluated using *Escherichia coli* (*E. coli*) and *Staphylococcus aureus* (*S. aureus*) cultivated in a trypticase soy broth (TSB) at 37  $^\circ\text{C}$  for 12 h. The bacterial cultures were adjusted to a concentration of  $10^6$  CFU/mL. Subsequently, TNTs, either uncoated or coated

with hydrogel films, were incubated in 1 mL of the bacterial suspension in TSB at 37  $^\circ\text{C}$  for 24 h. At the end of the incubation period, the concentration of bacteria in the culture medium was measured using optical density measurement at 625 nm with a spectrometric microplate reader.

**2.13. Statistical Analysis.** The data are expressed as the mean  $\pm$  the standard deviation (SD) of at least three independent experiments. Statistical analyses were performed using GraphPad Prism (GraphPad Software, USA). Significant differences among the multiple groups were determined by using one-way analysis of variance ANOVA. A *p* value  $<0.05$  was considered to be statistically significant.

### 3. RESULTS

**3.1. Physical Properties of the Hydrogel Films.** The PVA/gelatin hydrogel films synthesized with different ratios of PVA and gelatin, along with different concentrations of the glutaraldehyde cross-linker, showed distinct trends in the gel fraction. With a PL/G ratio of 50:50 and 0.1% glutaraldehyde cross-linker, the gel fraction was 68%. The gel fraction increased with a PL/G ratio of 25:75 and 0.2% glutaraldehyde cross-linker. Utilizing a PH/G ratio of 25:75 ratio and 0.2% glutaraldehyde cross-linker resulted in a larger gel fraction. Figure 1A show the gel fractions of each hydrogel film.

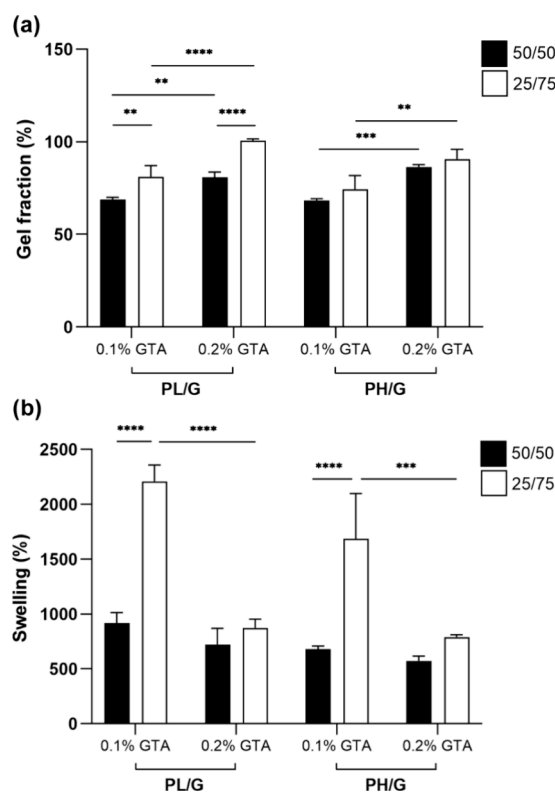


**Figure 1.** Physical properties of the PVA/gelatin hydrogel films: (a) Gel fraction; (b) Swelling. Data are presented as the mean  $\pm$  SD ( $n = 3$ ). \*\* $p \leq 0.01$ , \*\*\* $p \leq 0.001$ , \*\*\*\* $p \leq 0.0001$ .

The swelling behavior of the hydrogel films is shown in Figure 1B. The hydrogel films with a PVA/gelatin ratio of 25:75 exhibited a higher swelling percentage compared with those with a ratio of 50:50, regardless of the glutaraldehyde cross-linker concentration. Notably, when using 0.1% glutaraldehyde cross-linker, the films with a PL/G or PH/G ratio of

25:75 demonstrated the highest swelling percentages, surpassing suitable levels for optimal gelatin film formation. However, when using 0.2% glutaraldehyde cross-linker, the films with a PL/G or PH/G ratio of 25:75 exhibited optimal swelling behavior for gelatin film formation. Interestingly, when using 0.2% glutaraldehyde cross-linker, the swelling behavior was not significantly different between the PVA/gelatin ratios of 25:75 and 50:50 (for both PL/G and PH/G films). Based on the findings, the PL/G and PH/G films with 0.2% glutaraldehyde cross-linker were selected for further investigation.

### 3.2. FTIR Analysis of the PVA/Gelatin Hydrogel Films.

The FTIR spectra of the PVA/gelatin and glutaraldehyde cross-linker hydrogel films are shown in Figure 2. The PL/G

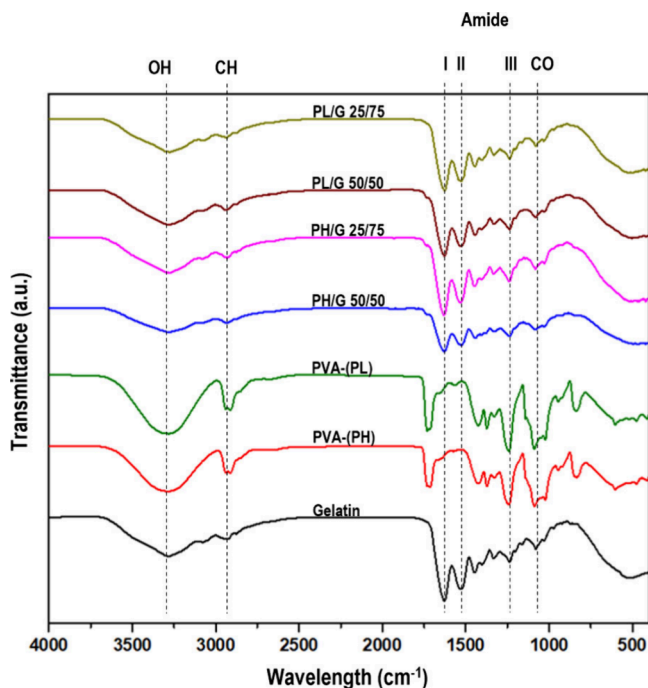


Figure 2. FTIR spectra of PVA, Gelatin and each formulation of PVA/gelatin hydrogel films.

25:75, PL/G 50:50, PH/G 25:75, and PH/G 50:50 hydrogel film FTIR spectra revealed absorption regions corresponding to the constituents of the hydrogel films. Specifically, absorption peaks indicative of gelatin were observed at approximately 1626.7, 1627.5, 1630.0, and 1627.8  $\text{cm}^{-1}$  for amide I; at 1526.1, 1525.3, 1535.7, and 1525.5  $\text{cm}^{-1}$  for amide II; and at 1237.0, 1238.0, 1238.5, and 1238.0  $\text{cm}^{-1}$  for amide III, respectively. Additionally, PVA exhibited broad peaks at 3273.5, 3273.2, 3273.3, and 3272.8  $\text{cm}^{-1}$ , indicating O–H stretching, as well as peaks at 2942.4, 2942.8, 2930.6, and 2935.1  $\text{cm}^{-1}$  for C–H vibrations, and 1080.5, 1081.0, 1081.4, and 1081.4  $\text{cm}^{-1}$  for C–O bond vibrations. Interestingly, there were slight changes in the absorption regions of gelatin and PVA in each hydrogel film formulation, attributed to the presence of the glutaraldehyde cross-linker.

**3.3. Cytotoxicity Evaluation of the PVA/Gelatin Hydrogel Films.** The PL/G and PH/G hydrogel films at ratios of 50:50 and 25:75 was evaluated for their cytotoxic effects. The PL/G 50:50 and PH/G 50:50 hydrogel films exerted toxicity. Specifically, the PL/G 50:50 hydrogel film led to significantly lower cell viability at the 100% and 50% concentrations compared with the control group. Similarly, the

PH/G 50:50 hydrogel film showed a decrease in cell viability at the 100% concentration. However, neither the PL/G 25:75 nor PH/G 25:75 hydrogel film exerted toxicity after 24 h of exposure (Figure 3).

**3.4. In Vitro Biodegradation.** The *in vitro* biodegradation test conducted on the PL/G 25:75 and PH/G 25:75 hydrogel films in PBS (pH 7.4) with lysozyme at 37 °C for 14 days presented significant results regarding the percentage change in the remaining weight (Figure 4). Initially, the PL/G hydrogel films exhibited a lower remaining weight than the PH/G hydrogel films after 24 h. On day 7, the PL/G and PH/G hydrogel films exhibited a decrease in the remaining weight. Subsequently, the degradation rate of the PL/G hydrogel films accelerated, surpassing that of the PH/G hydrogel films by day 14. These results indicate that the PH/G hydrogel films were more stable than the PL/G hydrogel films in the presence of enzymes.

**3.5. Structural Characterization of Vancomycin-Loaded TNTs Coated with Hydrogel Film.** The scanning electron micrographs in Figure 5 provide insights into the surface morphology of the uncoated TNTs and TNTs coated with hydrogel film. In the top-view scanning electron micrographs, the uncoated TNTs displayed a well-defined nanotubular surface with open tops and uniform diameters and structure. The TNTs had a pore diameter of  $<1 \mu\text{m}$ . In contrast, the TNTs coated with hydrogel film exhibited a distinct transformation in the surface characteristics. While the uncoated TNTs had a very rough and porous surface, the TNTs coated with hydrogel film had a smooth, nonporous surface. This transformation suggests successful coating of the TNT surface with PVA/gelatin hydrogel film. Furthermore, there were significant differences in the thickness of the PL/G and PH/G hydrogel films: The PH/G films were thicker than the PL/G films (Table 1). The use of high-viscosity PVA led to significant differences in the film volume compared with low-viscosity PVA, resulting in an increase in the average thickness of the hydrogel film.

**3.6. In Vitro Drug Release from Vancomycin-Loaded TNTs Coated with Hydrogel Film.** Figure 6 presents the release of vancomycin from vancomycin-loaded uncoated TNTs and TNTs coated with hydrogel film. Initially, uncoated TNTs exhibited a significant release of vancomycin within the first hour. In contrast, the cumulative release of vancomycin from TNTs coated with PL/G or PH/G hydrogel film was notably lower than that of uncoated TNTs and exhibited a gradual increase over time. Subsequently, the cumulative release of vancomycin stabilized at 48 h. Notably, the vancomycin release rate was uncoated vancomycin-loaded TNTs  $>$  vancomycin-loaded TNTs coated with PH/G hydrogel film  $>$  vancomycin-loaded TNTs coated with PL/G hydrogel films. These findings show that coating the surface of vancomycin-loaded TNTs with hydrogel film can effectively delay the release of vancomycin.

**3.7. Analysis of Glutaraldehyde Residues of Vancomycin-Loaded TNTs Coated with Hydrogel Film.** The glutaraldehyde residues in PH/G and PL/G films cross-linked using glutaraldehyde aimed to examine the potential toxicity associated with residual cross-linker. As shown in Table 2, the glutaraldehyde content was  $0.40 \pm 0.17 \mu\text{g}/\text{mg}$  for the PL/G hydrogel film and  $0.28 \pm 0.08 \mu\text{g}/\text{mg}$  for the PH/G hydrogel film. The amount of glutaraldehyde per piece of TNT coated with the PL/G hydrogel film ranged from  $44.87$  to  $67.82 \times 10^{-3}$ , while the amount of glutaraldehyde per piece of TNT

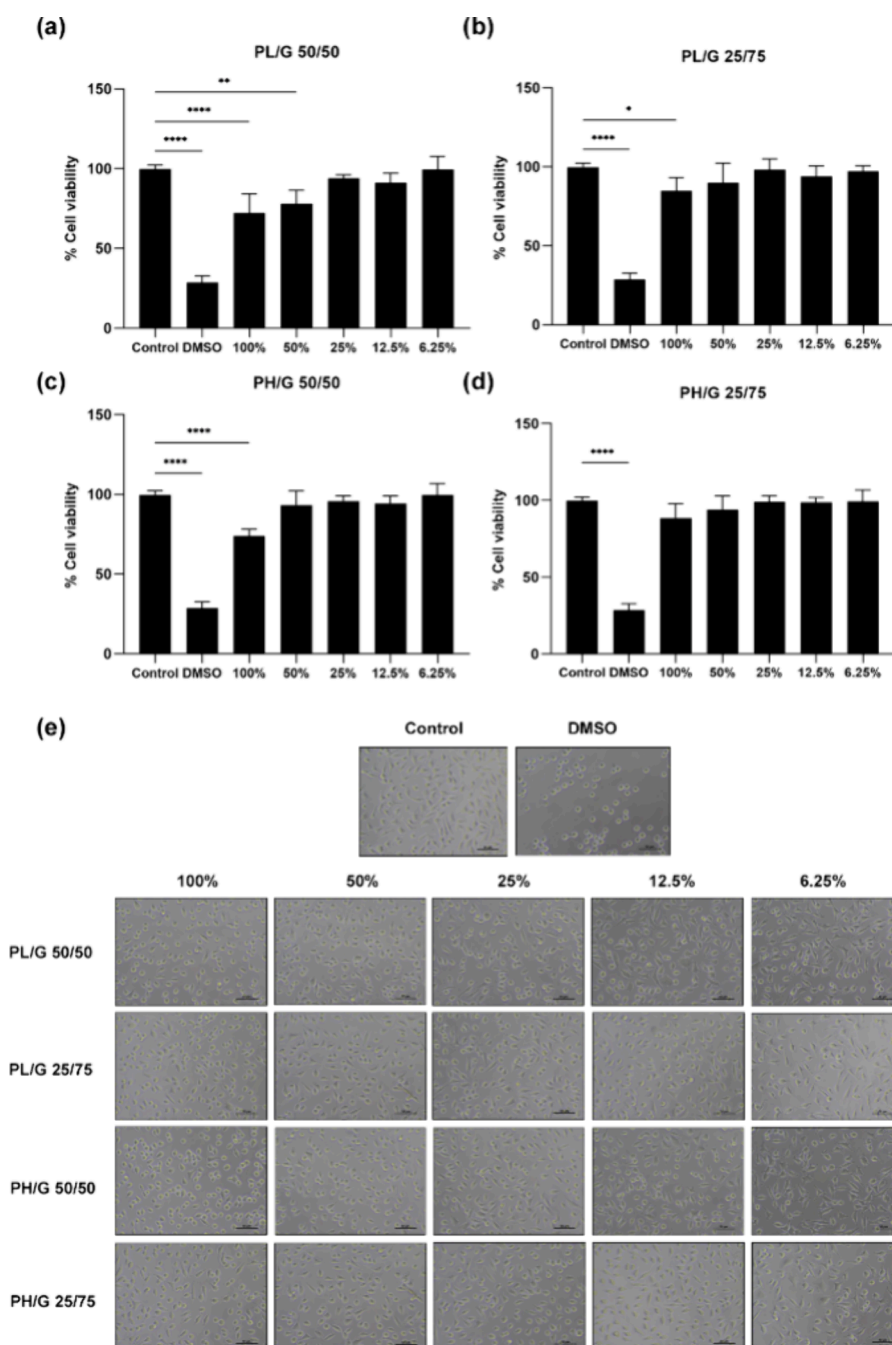


**Figure 3.** *In vitro* cytotoxicity and cell morphology observation of the extract media hydrogels toward L929 cells. MTT assay determined cytotoxicity profile of (a) PL/G 50/50, (b) PL/G 25/75, (c) PH/G 50/50, and (d) PH/G 25/75, and (e) cell morphology. Data are presented as the mean  $\pm$  SD ( $n = 3$ ). \* $p \leq 0.05$ , \*\* $p \leq 0.01$ , \*\*\*\* $p \leq 0.0001$ .

coated with the PH/G hydrogel film ranged from 7.26 to 12.06  $\times 10^{-3}$   $\mu\text{g}/\text{mg}$ .

**3.8. Cellular Behavior of Vancomycin-Loaded TNTs Coated with Hydrogel Film.** Exposure of MC3T3-E1 cells to uncoated TNTs or TNTs coated with the PH/G hydrogel film for 24 and 48 h did not lead to cytotoxicity (Figure 7). Conversely, there was a noticeable decrease in the viability of cells treated with the TNTs coated with the PL/G hydrogel film after 48 h. Subsequently, the growth of MC3T3-E1 bone cells was evaluated on the surface of vancomycin-loaded TNTs, uncoated or coated with PVA/gelatin hydrogel film, over a 7-day period. Remarkably, TNTs coated with the PH/G hydrogel film enhanced cell growth compared with uncoated

TNTs and TNTs coated with the PL/G hydrogel film (Figure 7B). Additionally, scanning electron micrographs showed adhered bone cells on the surface of vancomycin-loaded TNTs (Figure 7C), further confirming the biocompatibility and potential utility of hydrogel-coated TNTs in bone tissue engineering applications.

**3.9. Osteogenic Capacity of Vancomycin-Loaded TNTs Coated with PVA/Gelatin Hydrogel Film.** Assessment of the differentiation-inducing potential of TNTs coated with hydrogel film under osteogenic induction conditions involved measuring ALP activity and the calcium content. Osteoblasts grown on vancomycin-loaded TNTs coated with PVA/gelatin hydrogel film exhibited increased ALP activity

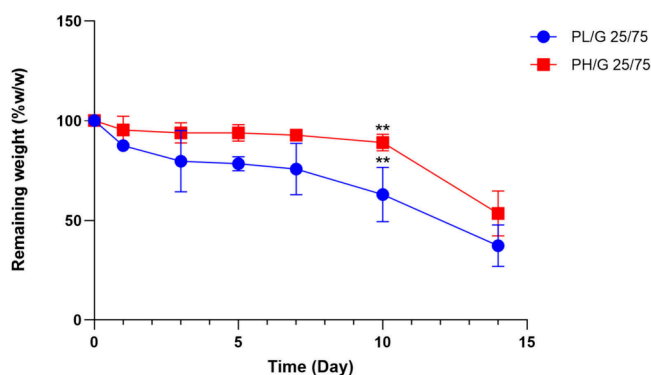


**Figure 4.** Remaining weight percentage of hydrogel films in phosphate buffer solution containing lysozyme enzyme at 37 °C for 14 days. Data are presented as the mean  $\pm$  SD ( $n = 4$ ). \*\*\* $p \leq 0.01$ .

and calcium accumulation at both 7 and 14 days compared with osteoblasts grown on uncoated TNTs (Figure 8). However, there were no significant differences in ALP activity and calcium content between the uncoated TNTs, TNTs coated with PH/G hydrogel film, and TNTs coated with PL/G hydrogel film.

### 3.10. Antibacterial Properties of Vancomycin-Loaded TNTs Coated with PVA/Gelatin Hydrogel Film.

The antibacterial properties of TNTs were evaluated to confirm the efficacy of the material following surface modification with hydrogel films. The concentrations of *E. coli* and *S. aureus* were significantly reduced in the presence of vancomycin-loaded TNTs coated with PVA/gelatin hydrogel films (Figure 9). Additionally, no significant differences in bacterial inhibition were observed between TNTs coated with PL/G and PH/G hydrogel film. These findings demonstrate the enhanced antibacterial properties of the hydrogel-coated vancomycin-loaded TNTs.

## 4. DISCUSSION

PVA and gelatin hydrogels have emerged as versatile biomaterials with significant potential across various biomedical applications. The combination of these two components result in hydrogel matrices with distinctive characteristics such as biocompatibility, adjustable mechanical

**Table 1.** Amount and Thickness of the Hydrogel Films Coated on the Vancomycin-Loaded TNTs<sup>a</sup>

Type of hydrogel films	Amount of hydrogel films (mg/cm <sup>2</sup> )	Thickness of hydrogel films ( $\mu$ m)
PL/G (25:75)	0.87 $\pm$ 0.41	27.89 $\pm$ 5.56*
PH/G (25:75)	1.38 $\pm$ 0.74	49.46 $\pm$ 10.64*

<sup>a</sup>Data are presented as the mean  $\pm$  SD ( $n = 3$ ). Values are significantly different compared between the PL/G and PH/G. \* $p \leq 0.05$ .

strength, and excellent water absorption capacity.<sup>19</sup> Additionally, they provide a biomimetic environment that supports cell growth, proliferation, and tissue regeneration, making them promising candidates for tissue engineering applications.<sup>12,14</sup> In this study, PVA/gelatin hydrogel films were synthesized successfully and cross-linked by glutaraldehyde. The cross-linking process between PVA and gelatin is essential in the fabrication of hydrogels. The cross-linking agent on the material enhances the mechanical strength and stability of the hydrogel matrix, making it more resistant to degradation and ensuring its structural integrity over time.<sup>20</sup> Moreover, cross-linking allows for the control of the hydrogel's properties, such as its swelling behavior and degradation rate.<sup>21–23</sup> Glutaraldehyde serves as a vital cross-linker in the fabrication of PVA/gelatin hydrogel films, playing a pivotal role in enhancing their mechanical strength, stability, and biocompatibility.<sup>21,24</sup> Previous studies have shown that cross-linking enhances the mechanical strength of hydrogels.<sup>25,26</sup> Adjusting the specific proportions of PVA/gelatin and cross-linking contribute advance biomaterials for biomedical applications.

The proportions of gelatin, PVA, and glutaraldehyde for hydrogel films plays an important role in determining the properties and performance of the resulting hydrogel. Different PVA/gelatin ratios result in different chemical and physical properties.<sup>27,28</sup> In the present study, higher concentrations of gelatin relative to PVA promoted stronger gel formation and a large gel fraction compared with lower concentrations of gelatin relative to PVA (Figure 1A). Gelatin contains natural peptide sequences that promote molecular interactions such as hydrogen bonding and electrostatic interactions, leading to gel formation. PVA was used to reinforce the shortcoming of gelatin, which is low mechanical strength.<sup>29</sup> Increasing the

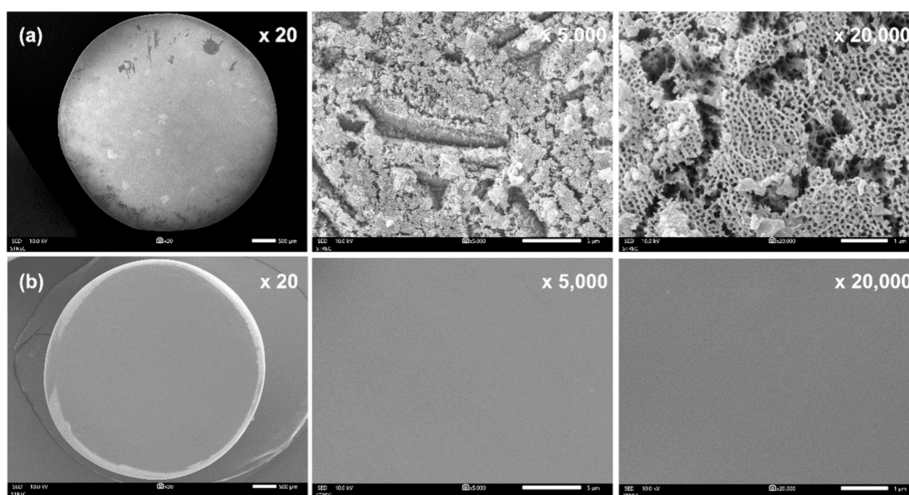


**Figure 5.** Representative SEM images for vancomycin-loaded TNTs surfaces of: (a) uncoated and (b) coated with PVA/gelatin hydrogel films.

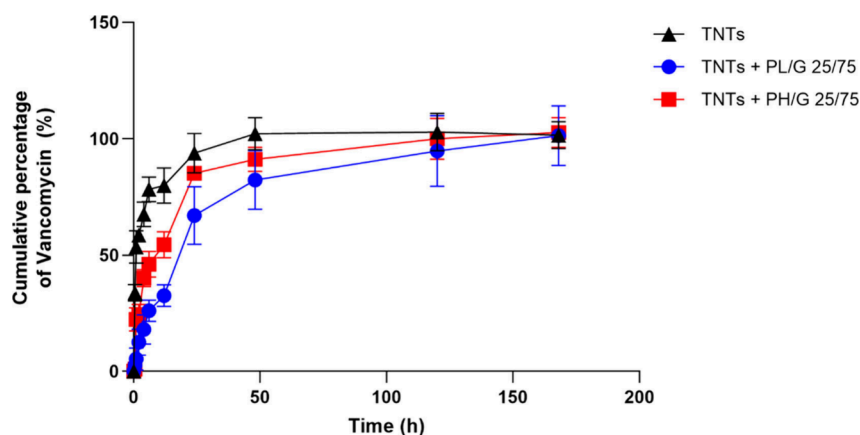


**Figure 6.** Cumulative percentage release of vancomycin from TNTs coated with hydrogel films. Data are presented as the mean  $\pm$  SD ( $n = 3$ ).

**Table 2.** Amount of Glutaraldehyde Residue in the PL/G and PH/G Hydrogel Films<sup>a</sup>

Type of hydrogel films	Amount of glutaraldehyde per hydrogel films ( $\mu\text{g}/\text{mg}$ film dry weight)	Amount of glutaraldehyde per piece of TNTs ( $\mu\text{g}/\text{kg}$ body weight)
PL/G 2S/7S	$0.40 \pm 0.17$	$44.87\text{--}67.82 \times 10^{-3}$
PH/G 2S/7S	$0.28 \pm 0.08$	$7.26\text{--}12.06 \times 10^{-3}$

<sup>a</sup>Data are presented as the mean  $\pm$  SD ( $n = 3$ ).

gelatin concentration provide more opportunities for these interactions to occur, resulting in a denser and more interconnected polymer network.<sup>28</sup> Furthermore, the homo-

geneity of PVA/gelatin scaffolds is improved as the gelatin concentration increases.<sup>30</sup> However, the hydrogel films made of PL/G or PH/G 2S:7S and 0.1% of glutaraldehyde showed excessive swelling (Figure 1B), suggesting an imbalance in the PVA/gelatin ratio and glutaraldehyde during hydrogel preparation. The amount of glutaraldehyde influences the mechanical performance of blended films.<sup>31</sup> Increasing the gelatin concentration increases the swelling ability.<sup>27</sup> FTIR was used to examine the chemical groups in the glutaraldehyde cross-linked PVA/gelatin hydrogel films. The FTIR spectra (Figure 2) showed the amide I peak (C = O stretching), the amide II peak (N–H bending and C–H stretching), and the amide III peak (C–N stretching plus N–H in phase bending),

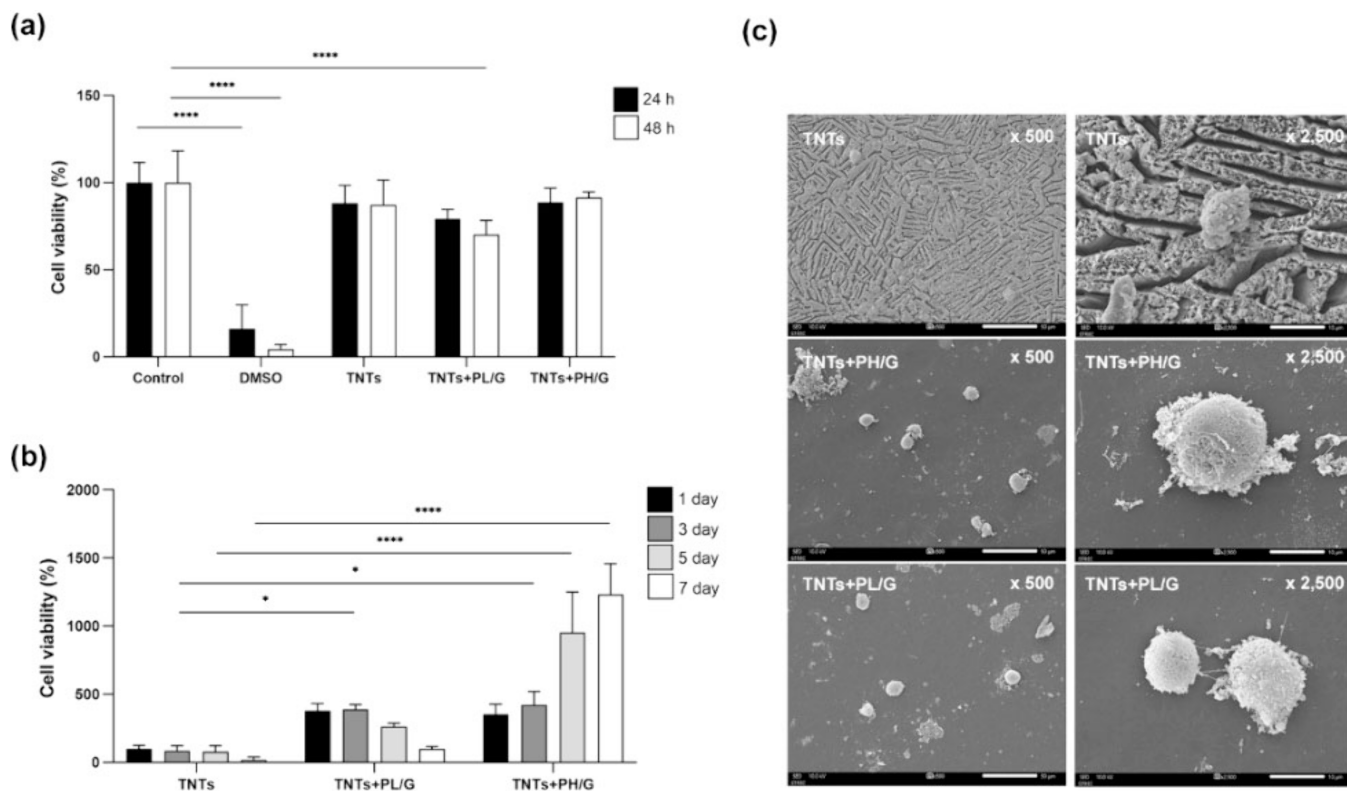


**Figure 7.** *In vitro* cytotoxicity of the vancomycin-loaded TNTs coated with PVA/gelatin hydrogel films toward MC3T3-E1 cells by CCK 8 assay. (a) Cell viability, (b) cell growth measurement using CCK 8 assay and (c) representative SEM images of adhered MC3T3-E1 cells on surface of vancomycin-loaded TNTs coated with PVA/gelatin hydrogel films. Data are presented as the mean  $\pm$  SD ( $n = 4$ ). \* $p \leq 0.05$ , \*\*\* $p \leq 0.0001$ .

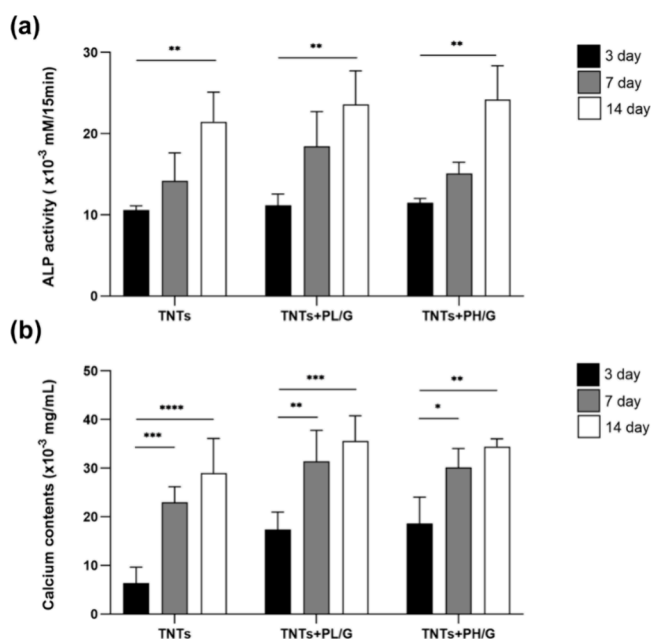


**Figure 8.** Osteogenic capacity of vancomycin-loaded TNTs coated with PVA/gelatin hydrogel films. (a) ALP activity and (b) calcium content in different groups under osteogenic medium after culture for 3, 7, and 14 days. Data are presented as the mean  $\pm$  SD ( $n = 4$ ). \* $p \leq 0.05$ , \*\* $p \leq 0.01$ , \*\*\* $p \leq 0.001$ , \*\*\*\* $p \leq 0.0001$ .

in accordance with previous studies.<sup>27,32</sup> Moreover, there were three peaks associated with the reaction between PVA and glutaraldehyde, consistent with a previous study.<sup>33</sup> There were minor shifts in the peak positions in the PVA and gelatin functional groups, which can be attributed to the cross-linking of various bonds during hydrogel formation.

Assessing cytotoxicity provides essential insights into the compatibility of hydrogel films with living cells, ensuring their safety for *in vivo* use. The PL/G 25:75 and PH/G hydrogel

films were not cytotoxic, but the PL/G 50:50 and PH/G 50:50 hydrogel films did exert some toxicity (Figure 3). In a previous study, hydrogels did not cause lysis of L-929 cells or exert toxicity.<sup>19</sup> Many studies have examined the safety of gelatin and PVA hydrogels in various cell types and have consistently reported no toxicity.<sup>12,34–37</sup> The integration of gelatin into synthetic polymers introduces various kinds of ligands capable of binding to receptors on the cell surface, thereby enhancing adhesion.<sup>12,19,34,38,39</sup> The data support safe and biocompatible PVA/gelatin formulation. These findings suggest that the cytotoxicity of PVA/gelatin hydrogel films is influenced by both the PVA/gelatin ratio and the concentration of the hydrogel, with lower ratios and concentrations demonstrating better biocompatibility with fibroblasts. Moreover, *in vitro* degradation indicated that the remaining weight percentage was higher for PH/G hydrogel films compared with PL/G hydrogel films (Figure 4). This finding underscores the differential degradation behavior of the PL/G and PH/G hydrogel films and highlights the importance of polymer composition in determining their biodegradation kinetics and stability in enzymatic environments. A possible explanation could be that high-viscosity PVA enhanced structural integrity and reduced the susceptibility of PVA to degradation. Consequently, the PH/G hydrogel films retained a greater proportion of their initial weight over time compared with the PL/G hydrogel films. A previous study showed that the viscosity of PVA affects the homogeneity of the polymer.<sup>40</sup>

A hydrogel film comprising PVA/gelatin cross-linked with glutaraldehyde was developed successfully to coat the surface of vancomycin-loaded TNTs, which were developed previously by our colleagues, offer a promising platform for controlled drug release.<sup>41</sup> *In vitro*, the vancomycin-loaded TNTs coated with PVA/gelatin hydrogel film presented controlled release of vancomycin. The incorporation of hydrogel film, particularly the PL/G hydrogel film, onto the surface of vancomycin-loaded TNTs delayed the release of vancomycin compared

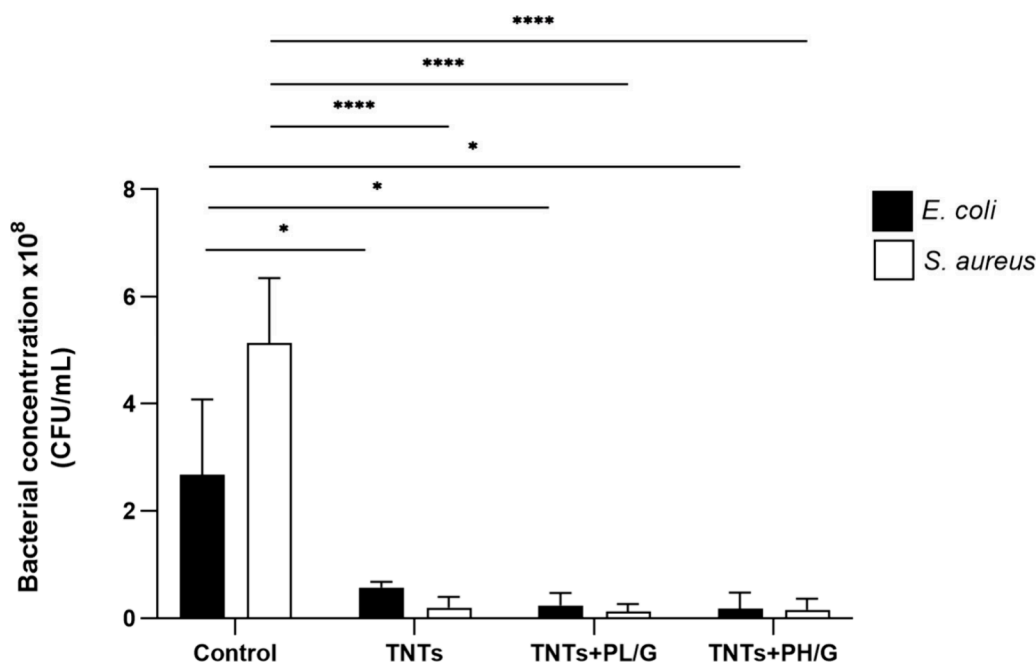


**Figure 9.** Antibacterial activity of vancomycin-loaded TNTs coated with PVA/gelatin hydrogel films. Bacterial concentrations of *E. coli* and *S. aureus* were measured in the medium after 24 h. Data are presented as the mean  $\pm$  SD ( $n = 3$ ). \* $p \leq 0.05$ , \*\*\*\* $p \leq 0.0001$ .



with the uncoated TNTs and the TNTs coated with the PH/G hydrogel film during the initial period. These findings suggest that the composition or structure of a hydrogel film, possibly influenced by factors such as polymer density or cross-linking density, plays a crucial role in modulating the release kinetics of vancomycin. Additionally, it is essential to analyze glutaraldehyde residues from PVA/gelatin hydrogel gels because residual cross-linker could potentially induce cytotoxic effects.<sup>42,43</sup> It is important to note that unstable glutaraldehyde polymers may be a contributing factor to toxicity concerns.<sup>44</sup> However, previous studies have demonstrated the non-cytotoxic nature of glutaraldehyde at certain concentrations.<sup>45,46</sup> Glutaraldehyde-cross-linked hydrogels using a concentration of 0.2% glutaraldehyde have been shown to exhibit biocompatibility in animal models.<sup>47</sup>

It was crucial to evaluate the osteogenic capacity of vancomycin-loaded TNTs coated with PVA/gelatin hydrogel film regarding their therapeutic potential in bone tissue engineering applications. ALP activity and calcium content are indicators used to evaluate the osteogenesis capacity of biomaterials. ALP is an early marker of osteogenic differentiation, reflecting the initial stages of bone formation. Increased ALP activity indicates the presence of osteoblasts and their commitment to bone tissue formation. On the other hand, calcium content serves as a late-stage marker of osteogenesis, representing the mineralization process characteristic of mature bone tissue.<sup>48</sup> Therefore, measuring ALP activity and calcium content provides insights into the progression of osteogenic differentiation induced by biomaterials. Although both TNTs+PH/G and TNTs+PL/G showed increased ALP activity and calcium content compared to TNTs alone, the differences were not statistically significant (Figure 8). These findings suggest that the potential synergistic effects of the hydrogel films coatings and the vancomycin-loaded TNTs to induce osteoblast related genes such as ALP, OCN, RUNX2, and collagen IA.<sup>49</sup> Moreover, TNTs regulate osteogenic differentiation of mesenchymal stem cells (MSCs) via crosstalk between MSCs and macrophages under oxidative stress.<sup>50</sup> Previous research has also shown that the size of TNTs affects bone formation capacity.<sup>50</sup>

The risk of infection following material implantation is a significant concern in biomedical applications, particularly in orthopedic and dental surgeries.<sup>51,52</sup> Implant-associated infections are highly relevant in terms of severity and the risk of treatment failure. *E. coli* (Gram-negative bacteria) and *S. aureus* (Gram-positive bacteria) are two common and clinically significant bacterial species. Both are known for their ability to form biofilms on surfaces, including medical implants, complicating treatment and increasing infection risks.<sup>51–55</sup> Vancomycin has been shown to be effective against a wide range of bacteria, significantly reducing the risk of biofilm formation.<sup>15,16,56</sup> Incorporating vancomycin into TNTs offers a promising strategy to mitigate infection risks postimplantation. The findings of this study indicate that the concentrations of *E. coli* and *S. aureus* were significantly reduced in the presence of vancomycin-loaded TNTs coated with hydrogel films compared to uncoated TNTs (Figure 9). This suggests that the hydrogel coating does not interfere the antibacterial efficacy of vancomycin. Previous studies have explored various strategies, such as coating implants with silver nanoparticles<sup>18,57</sup> or other antibiotics.<sup>58</sup> However, these approaches often come with significant disadvantages, particularly related to cytotoxicity.<sup>59,60</sup> The localized release of vancomycin from

the TNTs when coated with biocompatible hydrogel films can provide a sustained antibacterial effect directly at the implant site, thereby preventing the initial adhesion and proliferation of pathogenic bacteria. Further investigation into other biological evaluations, particularly *in vivo* studies, are warranted to comprehensively assess the biocompatibility and efficacy of the coated vancomycin-loaded TNTs compared with the uncoated material.

## 5. CONCLUSIONS

Overall, the integration of vancomycin-loaded TNTs coated with hydrogel film represents a versatile and effective not only enhance the antibacterial properties of vancomycin but also benefits from the biocompatibility and controlled release capabilities of hydrogel coatings, and clinical efficacy of biomedical implants.

## ■ ASSOCIATED CONTENT

### Supporting Information

The Supporting Information is available free of charge at <https://pubs.acs.org/doi/10.1021/acsomega.4c03942>.

Table S1 demonstrates the specific ratios of PVA, gelatin, and glutaraldehyde used to formulate the hydrogel films. These proportions were determined to optimize the biocompatibility, mechanical properties, and controlled drug release capabilities of the hydrogel coatings on vancomycin-loaded TNTs. The compositions are provided for different formulations used in the study. (PDF)

## ■ AUTHOR INFORMATION

### Corresponding Author

**Pornanong Aramwit** – Department of Pharmacy Practice, Faculty of Pharmaceutical Sciences and Center of Excellence in Bioactive Resources for Innovative Clinical Applications, Chulalongkorn University, Bangkok 10330, Thailand; The Academy of Science, The Royal Society of Thailand, Dusit, Bangkok 10330, Thailand; Faculty of Pharmacy, Silpakorn University, Nakhon Pathom 73000, Thailand; [orcid.org/0000-0001-7274-2431](https://orcid.org/0000-0001-7274-2431); Email: [aramwit@gmail.com](mailto:aramwit@gmail.com)

### Authors

**Thitima Wattanavijitkul** – Department of Pharmacy Practice, Faculty of Pharmaceutical Sciences and Center of Excellence in Bioactive Resources for Innovative Clinical Applications, Chulalongkorn University, Bangkok 10330, Thailand

**Jirapon Khamwannah** – Department of Metallurgical Engineering, Faculty of Engineering, Chulalongkorn University, Bangkok 10330, Thailand

**Boonrat Lohwongwatana** – Department of Metallurgical Engineering, Faculty of Engineering, Chulalongkorn University, Bangkok 10330, Thailand

**Chedtha Puncreobutr** – Department of Metallurgical Engineering, Faculty of Engineering, Chulalongkorn University, Bangkok 10330, Thailand

**Narendra Reddy** – Center for Incubation, Innovation, Research and Consultancy, Jyothy Institute of Technology, Bengaluru, Karnataka 560082, India

**Rungnapha Yamdech** – Department of Pharmacy Practice, Faculty of Pharmaceutical Sciences and Center of Excellence in Bioactive Resources for Innovative Clinical Applications, Chulalongkorn University, Bangkok 10330, Thailand

Sarocho Cherdchom – Department of Preventive and Social Medicine and Center of Excellence in Nanomedicine, Faculty of Medicine, Chulalongkorn University, Bangkok 10330, Thailand

Complete contact information is available at:  
<https://pubs.acs.org/10.1021/acsomega.4c03942>

### Author Contributions

T.W. conceived the experimental design of this study, and reviewed and revised the draft. J.K., B.L., C.P., N.R. and R.Y. carried out the experiments, data analysis and interpretation. S.C. carried out the conceptualization and writing—original draft. P.A. contributed to the design and implementation of the research and contributed to the final version of the manuscript. The manuscript was written through contributions of all authors. All authors have given approval to the final version of the manuscript.

### Notes

The authors declare no competing financial interest.

### ACKNOWLEDGMENTS

This research is funded by Thailand Science Research and Innovation Fund Chulalongkorn University (CU\_FRB65\_heh(50)\_059\_33\_03) and The National Research Council of Thailand.

### ABBREVIATIONS

ALP, alkaline phosphatase; CCK8, cell counting kit 8; CFU, colony forming unit; DI water, deionized water; DMEM, Dulbecco's modified eagle's medium; FTIR, Fourier-transform infrared; G, gelatin; HCL, hydrochloric acid; OCPC, o-cresolphthalein complex substrate; PBS, phosphate-buffered saline; PH, PVA high viscosity; PL, PVA low viscosity, PVA, poly(vinyl alcohol); SD, standard deviation; SDS, sodium dodecyl sulfate; SEM, Scanning electron microscopy; TNTs, titania nanotubes; TSB, tryptic soy broth

### REFERENCES

- (1) do Prado, R. F.; Esteves, G. C.; Santos, E. L. S.; Bueno, D. A. G.; Cairo, C. A. A.; Vasconcelos, L. G. O.; Sagnori, R. S.; Tessarin, F. B. P.; Oliveira, F. E.; Oliveira, L. D.; Villaca-Carvalho, M. F. L.; Henriques, V. A. R.; Carvalho, Y. R.; De Vasconcelos, L. M. R. In vitro and in vivo biological performance of porous Ti alloys prepared by powder metallurgy. *PLoS One* **2018**, *13* (5), No. e0196169.
- (2) Tian, P.; Liu, X. Surface modification of biodegradable magnesium and its alloys for biomedical applications. *Regen Biomater* **2015**, *2* (2), 135–51.
- (3) Verma, R. P. Titanium based biomaterial for bone implants: A mini review. *Materials Today: Proceedings* **2020**, *26*, 3148–3151.
- (4) Baltatu, M. S.; Vizureanu, P.; Sandu, A. V.; Solcan, C.; Hritcu, L. D.; Spataru, M. C. Research Progress of Titanium-Based Alloys for Medical Devices. *Biomedicines* **2023**, *11* (11), 2997.
- (5) Liu, J.; Liu, J.; Attarilar, S.; Wang, C.; Tamaddon, M.; Yang, C.; Xie, K.; Yao, J.; Wang, L.; Liu, C.; Tang, Y. Nano-Modified Titanium Implant Materials: A Way Toward Improved Antibacterial Properties. *Front Bioeng Biotechnol* **2020**, *8*, 576969.
- (6) Marin, E.; Lanzutti, A. Biomedical Applications of Titanium Alloys: A Comprehensive Review. *Materials (Basel)* **2024**, *17* (1), 114.
- (7) Xia, Y.; Feng, Z. C.; Li, C.; Wu, H.; Tang, C.; Wang, L.; Li, H. Application of additive manufacturing in customized titanium mandibular implants for patients with oral tumors. *Oncol Lett.* **2020**, *20* (4), 51.
- (8) Liu, L.; Bhatia, R.; Webster, T. J. Atomic layer deposition of nano-TiO(2) thin films with enhanced biocompatibility and

antimicrobial activity for orthopedic implants. *Int. J. Nanomedicine* **2017**, *12*, 8711–8723.

(9) Bashir, S.; Hina, M.; Iqbal, J.; Rajpar, A. H.; Mujtaba, M. A.; Alghamdi, N. A.; Wageh, S.; Ramesh, K.; Ramesh, S. Fundamental Concepts of Hydrogels: Synthesis, Properties, and Their Applications. *Polymers (Basel)* **2020**, *12* (11), 2702.

(10) DeMerlis, C. C.; Schoneker, D. R. Review of the oral toxicity of polyvinyl alcohol (PVA). *Food Chem. Toxicol.* **2003**, *41* (3), 319–26.

(11) Mahnama, H.; Dadbin, S.; Frounchi, M.; Rajabi, S. Preparation of biodegradable gelatin/PVA porous scaffolds for skin regeneration. *Artif Cells Nanomed Biotechnol* **2017**, *45* (5), 928–935.

(12) Thangprasert, A.; Tansakul, C.; Thuaksubun, N.; Meesane, J. Mimicked hybrid hydrogel based on gelatin/PVA for tissue engineering in subchondral bone interface for osteoarthritis surgery. *Materials & Design* **2019**, *183*, 108113.

(13) Zulkiflee, I.; Fauzi, M. B. Gelatin-Polyvinyl Alcohol Film for Tissue Engineering: A Concise Review. *Biomedicines* **2021**, *9* (8), 979.

(14) Salahuddin, B.; Wang, S.; Sangian, D.; Aziz, S.; Gu, Q. Hybrid Gelatin Hydrogels in Nanomedicine Applications. *ACS Appl. Bio Mater.* **2021**, *4* (4), 2886–2906.

(15) Edin, M. L.; Miclau, T.; Lester, G. E.; Lindsey, R. W.; Dahners, L. E. Effect of cefazolin and vancomycin on osteoblasts in vitro. *Clin Orthop Relat Res.* **1996**, *333* (333), 245–51.

(16) Rathbone, C. R.; Cross, J. D.; Brown, K. V.; Murray, C. K.; Wenke, J. C. Effect of various concentrations of antibiotics on osteogenic cell viability and activity. *J. Orthop Res.* **2011**, *29* (7), 1070–4.

(17) Matsuda, S.; Iwata, H.; Se, N.; Ikada, Y. Bioadhesion of gelatin films crosslinked with glutaraldehyde. *J. Biomed. Mater. Res.* **1999**, *45* (1), 20–27.

(18) Zhao, L.; Wang, H.; Huo, K.; Cui, L.; Zhang, W.; Ni, H.; Zhang, Y.; Wu, Z.; Chu, P. K. Antibacterial nano-structured titania coating incorporated with silver nanoparticles. *Biomaterials* **2011**, *32* (24), 5706–16.

(19) Jeong, H.; Lee, D. Y.; Yang, D. H.; Song, Y.-S. Mechanical and Cell-Adhesive Properties of Gelatin/Polyvinyl Alcohol Hydrogels and Their Application in Wound Dressing. *Macromol. Res.* **2022**, *30* (4), 223–229.

(20) Qin, Z.; Yu, X.; Wu, H.; Yang, L.; Lv, H.; Yang, X. Injectable and Cytocompatible Dual Cross-Linking Hydrogels with Enhanced Mechanical Strength and Stability. *ACS Biomater Sci. Eng.* **2020**, *6* (6), 3529–3538.

(21) Bigi, A.; Cojazzi, G.; Panzavolta, S.; Rubini, K.; Roveri, N. Mechanical and thermal properties of gelatin films at different degrees of glutaraldehyde crosslinking. *Biomaterials* **2001**, *22* (8), 763–8.

(22) Lou, X.; Chirila, T. V. Swelling behavior and mechanical properties of chemically cross-linked gelatin gels for biomedical use. *J. Biomater Appl.* **1999**, *14* (2), 184–91.

(23) Tian, Z.; Liu, W.; Li, G. The microstructure and stability of collagen hydrogel cross-linked by glutaraldehyde. *Polym. Degrad. Stab.* **2016**, *130*, 264–270.

(24) Akhtar, M. F.; Hanif, M.; Ranjha, N. M. Methods of synthesis of hydrogels... A review. *Saudi Pharm. J.* **2016**, *24* (5), 554–559.

(25) Ullah, S.; Hashmi, M.; Shi, J.; Kim, I. S. Fabrication of Electrospun PVA/Zein/Gelatin Based Active Packaging for Quality Maintenance of Different Food Items. *Polymers (Basel)* **2023**, *15* (11), 2538.

(26) Peng, Z.; Li, Z.; Zhang, F.; Peng, X. Preparation and Properties of Polyvinyl Alcohol/Collagen Hydrogel. *Journal of Macromolecular Science, Part B* **2012**, *51* (10), 1934–1941.

(27) Ceylan, S.; Gokturk, D.; Bolgen, N. Effect of crosslinking methods on the structure and biocompatibility of polyvinyl alcohol/gelatin cryogels. *Biomed Mater. Eng.* **2016**, *27* (4), 327–340.

(28) Pawde, S. M.; Deshmukh, K.; Parab, S. Preparation and characterization of poly(vinyl alcohol) and gelatin blend films. *J. Appl. Polym. Sci.* **2008**, *109* (2), 1328–1337.

(29) Kim, H.; Yang, G. H.; Choi, C. H.; Cho, Y. S.; Kim, G. Gelatin/PVA scaffolds fabricated using a 3D-printing process employed with a

low-temperature plate for hard tissue regeneration: Fabrication and characterizations. *Int. J. Biol. Macromol.* **2018**, *120*, 119–127.

(30) Choi, S. M.; Singh, D.; Kumar, A.; Oh, T. H.; Cho, Y. W.; Han, S. S. Porous Three-Dimensional PVA/Gelatin Sponge for Skin Tissue Engineering. *Int. J. Polym. Mater.* **2013**, *62* (7), 384–389.

(31) Wang, X.; Huang, Z.; Niu, Z.; Chen, F.; Liu, C. Glutaraldehyde Crosslinked High Content of Amylose/Polyvinyl Alcohol Blend Films with Potent Tensile Strength and Young's Modulus. *Polymers (Basel)* **2022**, *14* (24), 5550.

(32) Chang, M. C.; Ko, C. C.; Douglas, W. H. Conformational change of hydroxyapatite/gelatin nanocomposite by glutaraldehyde. *Biomaterials* **2003**, *24* (18), 3087–94.

(33) Figueiredo, K. C. S.; Alves, T. L. M.; Borges, C. P. Poly(vinyl alcohol) films crosslinked by glutaraldehyde under mild conditions. *J. Appl. Polym. Sci.* **2009**, *111* (6), 3074–3080.

(34) Barba, B. J. D.; Oyama, T. G.; Taguchi, M. Simple fabrication of gelatin-polyvinyl alcohol bilayer hydrogel with wound dressing and nonadhesive duality. *Polym. Adv. Technol.* **2021**, *32* (11), 4406–4414.

(35) Masri, S.; Maarof, M.; Mohd, N. F.; Hiraoka, Y.; Tabata, Y.; Fauzi, M. B. Injectable Crosslinked Genipin Hybrid Gelatin-PVA Hydrogels for Future Use as Bioinks in Expediting Cutaneous Healing Capacity: Physicochemical Characterisation and Cytotoxicity Evaluation. *Biomedicine* **2022**, *10* (10), 2651.

(36) Elango, J.; Zamora-Ledezma, C.; Negrete-Bolagay, D.; Aza, P. N.; Gomez-Lopez, V. M.; Lopez-Gonzalez, I.; Belen Hernandez, A.; De Val, J.; Wu, W. Retinol-Loaded Poly(vinyl alcohol)-Based Hydrogels as Suitable Biomaterials with Antimicrobial Properties for the Proliferation of Mesenchymal Stem Cells. *Int. J. Mol. Sci.* **2022**, *23* (24), 15623.

(37) Corona-Escalera, A. F.; Tinajero-Diaz, E.; Garcia-Reyes, R. A.; Luna-Barcenas, G.; Seyfoddin, A.; Padilla-de la Rosa, J. D.; Gonzalez-Avila, M.; Garcia-Carvajal, Z. Y. Enzymatic Crosslinked Hydrogels of Gelatin and Poly (Vinyl Alcohol) Loaded with Probiotic Bacteria as Oral Delivery System. *Pharmaceutics* **2022**, *14* (12), 2759.

(38) Su, K.; Wang, C. Recent advances in the use of gelatin in biomedical research. *Biotechnol. Lett.* **2015**, *37* (11), 2139–45.

(39) Oyama, T. G.; Oyama, K.; Kimura, A.; Yoshida, F.; Ishida, R.; Yamazaki, M.; Miyoshi, H.; Taguchi, M. Collagen hydrogels with controllable combined cues of elasticity and topography to regulate cellular processes. *Biomed Mater.* **2021**, *16* (4), 045037.

(40) Kotoky, T.; Dolui, S.K. Synthesis and Characterisation of Polyvinyl alcohol (PVA)/Silica Hybrid Composites Derived Through the Sol-Gel Method in Aqueous Medium: Effect of Acid Content, Silica Content and Viscosity of PVA on the Dispersion Characteristics of Silica and the Physical Properties of the Composites. *J. Sol-Gel Sci. Technol.* **2004**, *29*, 107–114.

(41) Chunate, H. T.; Khamwannah, J.; Aliyu, A. A. A.; Tantavisut, S.; Puncreobutr, C.; Khamkongkao, A.; Tongyam, C.; Tumkhanon, K.; Phetrattanarangsi, T.; Chanamuangkon, T.; Sitthiwani, T.; Decha-Umphai, D.; Pongjirawish, P.; Lohwongwatana, B. Titania Nanotube Architectures Synthesized on 3D-Printed Ti-6Al-4V Implant and Assessing Vancomycin Release Protocols. *Materials (Basel)* **2021**, *14* (21), 6576.

(42) Zeiger, E.; Gollapudi, B.; Spencer, P. Genetic toxicity and carcinogenicity studies of glutaraldehyde—a review. *Mutat. Res.* **2005**, *589* (2), 136–51.

(43) Gough, J. E.; Scotchford, C. A.; Downes, S. Cytotoxicity of glutaraldehyde crosslinked collagen/poly(vinyl alcohol) films is by the mechanism of apoptosis. *J. Biomed Mater. Res.* **2002**, *61* (1), 121–30.

(44) Huang-Lee, L. L.; Cheung, D. T.; Nimni, M. E. Biochemical changes and cytotoxicity associated with the degradation of polymeric glutaraldehyde derived crosslinks. *J. Biomed Mater. Res.* **1990**, *24* (9), 1185–201.

(45) Umashankar, P. R.; Mohanan, P. V.; Kumari, T. V. Glutaraldehyde treatment elicits toxic response compared to decellularization in bovine pericardium. *Toxicol Int.* **2012**, *19* (1), 51–8.

(46) Reddy, N.; Reddy, R.; Jiang, Q. Crosslinking biopolymers for biomedical applications. *Trends Biotechnol.* **2015**, *33* (6), 362–9.

(47) Wu, X.; Black, L.; Santacana-Laffitte, G.; Patrick, C. W., Jr Preparation and assessment of glutaraldehyde-crosslinked collagen-chitosan hydrogels for adipose tissue engineering. *J. Biomed Mater. Res. A* **2007**, *81* (1), 59–65.

(48) Lee, J. S.; Kim, M. E.; Seon, J. K.; Kang, J. Y.; Yoon, T. R.; Park, Y. D.; Kim, H. K. Bone-forming peptide-3 induces osteogenic differentiation of bone marrow stromal cells via regulation of the ERK1/2 and Smad1/5/8 pathways. *Stem Cell Res.* **2018**, *26*, 28–35.

(49) Kang, H.; Dong, Y.; Liu, H.; Luo, C.; Song, H.; Zhu, M.; Guo, Q.; Peng, R.; Li, F.; Li, Y. Titania-Nanotube-Coated Titanium Substrates Promote Osteogenesis and Suppress Osteoclastogenesis via Integrin  $\alpha$ 5 $\beta$ 3. *ACS Appl. Bio Mater.* **2022**, *5* (12), 5832–5843.

(50) Shen, X.; Yu, Y.; Ma, P.; Luo, Z.; Hu, Y.; Li, M.; He, Y.; Zhang, Y.; Peng, Z.; Song, G.; Cai, K. Titania nanotubes promote osteogenesis via mediating crosstalk between macrophages and MSCs under oxidative stress. *Colloids Surf. B Biointerfaces* **2019**, *180*, 39–48.

(51) Zimmerli, W.; Sendi, P. Pathogenesis of implant-associated infection: the role of the host. *Semin Immunopathol* **2011**, *33* (3), 295–306.

(52) Pye, A. D.; Lockhart, D. E.; Dawson, M. P.; Murray, C. A.; Smith, A. J. A review of dental implants and infection. *J. Hosp Infect* **2009**, *72* (2), 104–10.

(53) Cremet, L.; Corvec, S.; Bemer, P.; Bret, L.; Lebrun, C.; Lesimple, B.; Miegerville, A. F.; Reynaud, A.; Lepelletier, D.; Caroff, N. Orthopaedic-implant infections by *Escherichia coli*: molecular and phenotypic analysis of the causative strains. *J. Infect* **2012**, *64* (2), 169–75.

(54) Giannelli, M.; Landini, G.; Materassi, F.; Chellini, F.; Antonelli, A.; Tani, A.; Zecchi-Orlandini, S.; Rossolini, G. M.; Bani, D. The effects of diode laser on *Staphylococcus aureus* biofilm and *Escherichia coli* lipopolysaccharide adherent to titanium oxide surface of dental implants. An in vitro study. *Lasers Med. Sci.* **2016**, *31* (8), 1613–1619.

(55) Nandakumar, V.; Chittaranjan, S.; Kurian, V. M.; Doble, M. Characteristics of bacterial biofilm associated with implant material in clinical practice. *Polym. J.* **2013**, *45* (2), 137–152.

(56) Wu, C. L.; Hsueh, J. Y.; Yip, B. S.; Chih, Y. H.; Peng, K. L.; Cheng, J. W. Antimicrobial Peptides Display Strong Synergy with Vancomycin Against Vancomycin-Resistant *E. faecium*, *S. aureus*, and Wild-Type *E. coli*. *Int. J. Mol. Sci.* **2020**, *21* (13), 4578.

(57) De Giglio, E.; Cafagna, D.; Cometa, S.; Allegratta, A.; Pedico, A.; Giannossa, L. C.; Sabbatini, L.; Mattioli-Belmonte, M.; Iatta, R. An innovative, easily fabricated, silver nanoparticle-based titanium implant coating: development and analytical characterization. *Anal Bioanal Chem.* **2013**, *405* (2–3), 805–16.

(58) Tiwari, A.; Sharma, P.; Vishwamitra, B.; Singh, G. Review on Surface Treatment for Implant Infection via Gentamicin and Antibiotic Releasing Coatings. *Coatings* **2021**, *11* (8), 1006.

(59) Haugen, H. J.; Makhtari, S.; Ahmadi, S.; Hussain, B. The Antibacterial and Cytotoxic Effects of Silver Nanoparticles Coated Titanium Implants: A Narrative Review. *Materials (Basel)* **2022**, *15* (14), 5025.

(60) Xie, C. M.; Lu, X.; Wang, K. F.; Meng, F. Z.; Jiang, O.; Zhang, H. P.; Zhi, W.; Fang, L. M. Silver nanoparticles and growth factors incorporated hydroxyapatite coatings on metallic implant surfaces for enhancement of osteoinductivity and antibacterial properties. *ACS Appl. Mater. Interfaces* **2014**, *6* (11), 8580–9.